Large Tunable, THz Electro-Optic Response in Cadmium Manganese Telluride (Cd,Mn)Te Single Crystals

Cadmium manganese telluride (Cd,Mn)Te (CMT) is a well-studied II–VI semiconductor because of its many desirable attributes and versatility. One such attribute is CMT's stable zinc-blend structure for Mn concentrations, x, up to 0.70, providing a very wide tuning range of the energy bandgap E_g. CMT also exhibits a large magneto-optic Faraday effect and is commonly used for isolators. Finally, it has a very high stopping power, showing great potential for x- and γ-ray detection.[1,2] In this article, we demonstrate CMT's exceptionally large electro-optic (EO) Pockels effect, which has previously been underestimated because of screening of the applied electric field by free carriers. Furthermore, we discuss how the EO sensitivity can be magnified for a particular operating probe wavelength using bandgap engineering.

Electro-optic sampling (EOS) measurements were performed using a modified configuration of that described by Zheng *et al.*,[3] in which the transmitted beam was collected. The subpicosecond pulses for all measurements were generated by a low-temperature–grown GaAs, freestanding photoconductive switch (PCS) integrated onto a coplanar strip (CS) transmission line.[4] Our CMT samples were as-grown, millimeter-size single crystals obtained using a modified vertical Bridgman method.[1] The crystals were oriented in such a manner that the electric field was applied along the [110] direction, and the sampling beam, incident along the [–110] direction, had parallel polarization with respect to the electric field. This configuration ensured maximum EO interaction.[5]

Since CMT is a semi-magnetic semiconductor, it was important to determine first whether the CMT optical response was a result of the EO Pockels effect or the magneto-optic Faraday effect. The PCS element was positioned at the center of the CS line, while the CMT transducer was placed on the transmission line, to one side of the PCS at first, and moved to the other side of the switch in a second measurement. This way the electric field of the signal generated by the PCS was constant on both ends of the CS line. However, the polarity of the magnetic field was flipped. The measurements showed no sign change of the signal, establishing that the dominant mechanism in sampling an ultrafast signal is the EO effect.

EO transducers are able to resolve THz pulses by converting the electric field into a retardation Γ of the sampling beam's polarization. For x-cut $LiTaO_3$, Γ is given by

$$\Gamma_{LTO} = \frac{2\pi(n_e - n_o)L_1}{\lambda} - \frac{\pi\left(n_e^3 r_{33} - n_o^3 r_{13}\right)L_2}{\lambda d} V_{LTO}, \qquad (1)$$

where the non-isotropic $LiTaO_3$ has two significant EO coefficients, r_{33} and r_{13}, and an extraordinary and ordinary refractive index, n_e and n_o, respectively. The gap between transmission lines is d, the crystal thickness is L_1, the interaction length between crystal and electric field is L_2, and V_{LTO} is the voltage transient propagating beneath the $LiTaO_3$ crystal. It is important to note that this transient is affected by the dielectric of the measuring transducer. The first term of the Γ_{LTO} equation is the intrinsic birefringence independent of the electric field and can be negated by a second perpendicular crystal of equal L_1. The second term is the Pockels-induced birefringence.

Isotopic $\bar{4}$3m crystals have no intrinsic birefringence, so Γ of the CMT transducer is[6]

$$\Gamma_{CMT} = \frac{2\pi\left(n_o^3 r_{41}\right)L_2}{\lambda d} V_{CMT}, \qquad (2)$$

where V_{CMT} is the CMT counterpart to V_{LTO} and the only nonzero components of the EO tensor are $r_{41} = r_{52} = r_{63}$. Literature[6] for CdTe gives $r_{41} = 4.5$ pm/V, which is based on measurements taken at $\lambda = 1$ μm and for frequencies lower than 20 kHz. Assuming that the refractive indices and EO coefficients for $LiTaO_3$ (Ref. 7) are constant in the 633- to 800-nm wavelength range, calculations show that Γ_{CMT} is less than Γ_{LTO}. This is, however, in direct contradiction to our experimental results shown in Fig. 125.35, where we present the

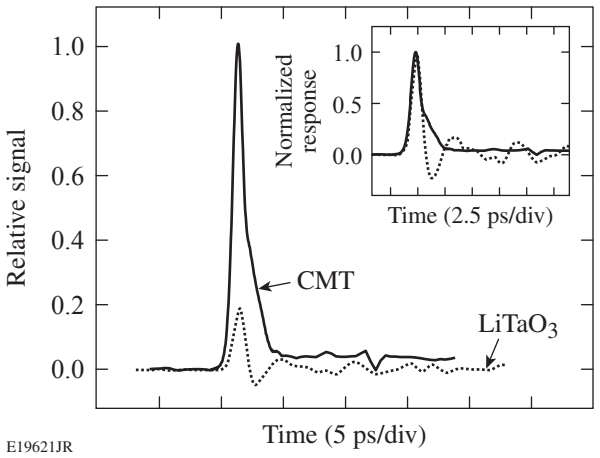

Figure 125.35
EOS response of a 1.45-V pulse detected by $Cd_{0.88}Mn_{0.12}Te$ (solid) and $LiTaO_3$ (dotted) transducers at a sampling beam wavelength of 800 nm. The inset compares the normalized responses of CMT (solid) and $LiTaO_3$ (dotted).

EO sampling responses of a $Cd_{0.88}Mn_{0.12}Te$ transducer (solid) and the widely used EO crystal $LiTaO_3$ (dotted). We see that CMT exhibits retardation five times greater than that of $LiTaO_3$.

The differential transfer function for the EO modulator in our setup is

$$\frac{\Delta V}{V_0} = \frac{1}{2}\sin\left(\pi V / V_\pi\right) \approx \frac{\pi V}{2V_\pi}, \quad \text{for } V \ll V_\pi , \tag{3}$$

where V_π is the V_{LTO} required to retard the optical probe by π and the dc component (V_0) is 31.5 mV/μW times the measured power of the transmitted probe. It is not possible, however, to determine the magnitude of r_{41} directly from the CMT EOS response because of the unknown variables L_2 and V_{CMT}. Therefore, we first determined the coupling between the transducer and transmission line using $LiTaO_3$. Coupling measurements were easily accomplished by directly applying a 2-V peak-to-peak, low-frequency (MHz) sinusoid, bypassing the PCS entirely. Knowing the EO coefficients for $LiTaO_3$ (Ref. 6), V_{LTO} and L_2 were calculated from the EOS response and coupling measurements using Eqs. (1) and (3).

The L_2 was small (1.18±0.26 μm), which we assume was a result of the poor condition of the substrate. This was confirmed by calculating a large air gap of 24 μm between the transmission line and crystal. These calculations were determined by the impedance for our CS line in a multilayer substrate[8] ($LiTaO_3$/air-gap/MgO) using the effective dielectric $\varepsilon_{eff} = (c/v)^2 = 9.2$. The velocity v was evaluated using the temporal delay of the EOS response measured for two spots with a known spatial separation. The ε_{eff} also established the reflection of the pulse at the crystal interface along the transmission line. The impedance mismatch in $LiTaO_3$ resulted in a 14% reflection of the generated pulse at the crystal interface, and the original signal of the PCS was then obtained (~1.45 V). Finally, the same air gap for CMT resulted in a smaller (3.5%) reflection, showing that V_{CMT} was $1.12 \times V_{LTO}$.

We strongly believe that the discrepancy between our ultrafast CMT retardation value and the low-frequency one given in the literature is caused by free carriers present in as-grown CMT crystals. These crystals are naturally *p*-type and holes are capable of screening slow oscillations of applied voltage, preventing any significant EO coupling at low frequencies. The free-carrier screening frequency can be estimated by dividing our CMT sample conductivity $\sigma \approx 10^{-3}$ S/cm (Ref. 1) by its permittivity, resulting in a value as high as 1.25 GHz. Measuring the EO response at 256 kHz, we calculated that the suppressed r_{41} for $Cd_{0.88}Mn_{0.12}Te$ was as low as 2.7±0.8 pm/V. This result was in close approximation to CdTe [4.5 pm/V (Ref. 6)] and $Cd_{0.75}Mn_{0.25}Te$ [3.5 pm/V (Ref. 8)] coefficients found in literature.

The fact that our CMT transducer was able to render the ultrafast PCS signal precisely (Fig. 125.35) with the response 5× greater (ΔV = 504 μV) than that of $LiTaO_3$ (ΔV = 95 μV) is because the pulse generated by the switch contains frequency components far exceeding the carrier screening process.

Table 125.II provides the *r* coefficients and the V_π values for several CMT crystals, taking into account the previously calculated coupling factors and the wavelength-dependent n_0, as well as the other EO transducers found in the literature. Comparative measurements in Table 125.II for $Cd_{0.82}Mn_{0.12}Te$ and $Cd_{0.91}Mn_{0.09}Te$ show that the kHz- and MHz-range measurements undervalue the EO coefficient by nearly an order of magnitude because of screening effects. Furthermore, our independent EO coupling measurements performed on $Cd_{0.91}Mn_{0.09}Te$ at 256 kHz but at 10 K, demonstrated that the EO response was 10× greater than that at 300 K. In the latter case, free carriers were immobilized by deep-level traps as the temperature was lowered.

EOS measurements for various wavelengths were performed using a $Cd_{0.91}Mn_{0.09}Te$ crystal (Fig. 125.36), showing a dramatic increase of the EO response when approaching E_g. Knowing that the signal is electro-optic in nature, we attributed

Table 125.II: Measurements (bold) and previously reported values of the optimum EO coefficients and V_π for several (Cd,Mn)Te crystals of x and for other popular EO transducers. Provided are the probe wavelength, tested signal frequency, and the probe wavelength appropriate n for the crystal.

Crystal	λ (nm)	f	n	r (pm/V)	$V_\pi \cdot d/L_2$ (V)
CdTe	**855**	**THz**	$\mathbf{n_o = 2.91}$	$\mathbf{r_{41} = 30.2 \pm 2.9}$	**572**
CdTe (Ref. 6)	1000	kHz	$n_o = 2.84$	$r_{41} = 4.5$	3880
$\mathbf{Cd_{0.91}Mn_{0.09}Te}$	**855**	**THz**	$\mathbf{n_o = 2.76}$	$\mathbf{r_{41} = 24.7 \pm 1.2}$	**821**
$\mathbf{Cd_{0.88}Mn_{0.12}Te}$	**800**	**THz**	$\mathbf{n_o = 2.79}$	$\mathbf{r_{41} = 28.3 \pm 5.9}$	**651**
$\mathbf{Cd_{0.88}Mn_{0.12}Te}$	**800**	**kHz**	$\mathbf{n_o = 2.79}$	$\mathbf{r_{41} = 2.7 \pm 0.8}$	**6825**
$Cd_{0.75}Mn_{0.25}Te$ (Ref. 8)	800	GHz	$n_o = 2.64$	$r_{41} = 3.5 \pm 0.5$	4735
$\mathbf{Cd_{0.50}Mn_{0.50}Te}$	**855**	**THz**	$\mathbf{n_o = 2.52}$	$\mathbf{r_{41} = 25.3 \pm 1.2}$	**1059**
$LiTaO_3$ (Ref. 6)	800	THz	$n_{e/o} = 2.18/2.176$	$r_{33/13} = 33/7.5$	3490
ZnTe (Ref. 12)	800	THz	$n_o = 3.24$	$r_{41} = 4.04$	2911
DAST (Ref. 3)	810	THz	$n_{a/b} = 2.46/1.68$	$r_{11/21} = 77/42$	790

this phenomenon to the wavelength dependence of n_o (Ref. 9). Our experimental EOS dependence on wavelength was fit (solid line in Fig. 125.36) using the $n(\lambda)$ dispersion model given by Schubert *et al.*[10] Taking the asymptote as the crystal bandgap, the E_g (1.623 eV) was slightly smaller than the calculated value [1.646 eV (Ref. 11)], apparently, because of interstitial states broadening the bandgap. The EO dependence on λ can be easily exploited by either tuning the operating probe λ to near-E_g, as we have presented in Fig. 125.36. Alternatively, for tests using a fixed probe wavelength above 600 nm, crystals can be custom grown to match for greatest signal quality. We finally note that Table 125.II shows that for an 855-nm probe, CdTe has twice the sensitivity as $Cd_{0.50}Mn_{0.50}Te$, but the CdTe bandgap limits its practical use to $\lambda > 812$ nm.

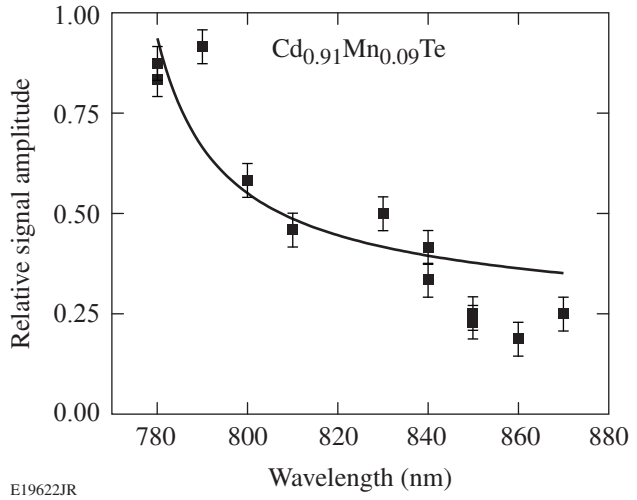

Figure 125.36
Wavelength dependence of $Cd_{0.91}Mn_{0.09}Te$ EO effect. Fittings are based on $n(\lambda)$ dispersion (solid line).

The calibration method used here allowed us to obtain absolute values of the EO coefficient for tested CMT crystals. We have demonstrated that, ultimately, CMT is significantly more sensitive at THz frequencies than previously expected[12] and more sensitive than the widely used indirect EO crystal $LiTaO_3$; the typical free-space THz EO transducer ZnTe;[12] and even when compared to DAST, an organic crystal exhibiting the largest EO coefficient of any material.[3,13] Furthermore, CMT exhibits a low ε_r, so only a small percentage of the signal is lost because of reflections along the transmission line. The CMT EOS response shown in Fig. 125.35 also presents a much cleaner signal as compared to the $LiTaO_3$ response because of the absence of a significant dielectric loading. Carrier screening was verified as the source of an order-of-magnitude difference between the CMT EO effect response at very high (THz) and low (MHz) frequencies. Finally, the CMT EO wavelength dependence was exploited to garner the highest sensitivity.

ACKNOWLEDGMENT

The authors thank Drs. W. R. Donaldson and H. Irie for their many valuable discussions. A. S. C. acknowledges support from the Frank Horton Graduate Fellowship Program at the University of Rochester Laboratory for Laser Energetics. Work in Rochester was supported in part by NSF grant No. ECCS-0901701 and the U.S. Department of Energy Office of Inertial Confinement Fusion under Cooperative Agreement No. DE-FC 52-08NA28302, the University of Rochester, and the New York State Energy Research and

Development Authority. The support of DOE does not constitute an endorsement by DOE of the views expressed in this article. Work in Warsaw was supported by the Polish Ministry of Science and Higher Education through grant 3 T08A 046 30.

REFERENCES

1. A. Mycielski *et al*., Phys. Stat. Sol. (C) **2**, 1578 (2005).
2. A. S. Cross, J. P. Knauer, A. Mycielski, D. Kochanowska, M. Wiktowska-Baran, R. Jakieła, J. Domagała, Y. Cui, R. B. James, and R. Sobolewski, Nucl. Instrum. Methods Phys. Res. A **624**, 649 (2010).
3. X. Zheng, S. Wu, R. Sobolewski, R. Adam, M. Mikulics, P. Kordoš, and M. Siegel, Appl. Phys. Lett. **82**, 2383 (2003).
4. R. Adam, M. Mikulics, A. Förster, J. Schelten, M. Siegel, P. Kordoš, X. Zheng, S. Wu, and R. Sobolewski, Appl. Phys. Lett. **81**, 3485 (2002).
5. S. Namba, J. Opt. Soc. Am. **51**, 76 (1961).
6. A. Yariv, *Optical Electronics in Modern Communications*, 5th ed., The Oxford Series in Electrical and Computer Engineering (Oxford University Press, New York, 1997).
7. Q. Wu and X.-C. Zhang, Appl. Phys. Lett. **68**, 1604 (1996).
8. E. Chen and S. Y. Chou, IEEE Trans. Microw. Theory Tech. **45**, 939 (1997).
9. A. S. Cross, D. Wang, G. Guarino, S. Wu, A. Mycielski, and R. Sobolewski, J. Phys., Conf. Ser. **92**, 012015 (2007).
10. D. W. Schubert *et al*., Appl. Phys. Lett. **60**, 2192 (1992).
11. J. K. Furdyna, J. Appl. Phys. **64**, R29 (1988).
12. B. Pradarutti *et al*., Opt. Commun. **281**, 5031 (2008).
13. F. Pan *et al*., Appl. Phys. Lett. **69**, 13 (1996).